

1 **Tribological evaluation of a novel hybrid for repair of articular cartilage defects**

2 Maria Parkes¹, Francesca Tallia², Gloria R. Young², Philippa Cann¹, Julian R. Jones², Jonathan R. T.
3 Jeffers¹

4 ¹ Department of Mechanical Engineering, Imperial College London, South Kensington Campus,
5 London, SW7 2AZ, UK

6
7 ² Department of Materials, Imperial College London, South Kensington Campus, London, SW7 2AZ,
8 Uk

9

10 Abstract

11 The friction and wear properties of silica/poly(tetrahydrofuran)/poly(ϵ -caprolactone)
12 (SiO_2 /PTHF/PCL-diCOOH) hybrid materials that are proposed as cartilage tissue engineering materials
13 were investigated against living articular cartilage. A testing rig was designed to allow testing against
14 fresh bovine cartilage. The friction force and wear were compared for five compositions of the
15 hybrid biomaterial articulating against freshly harvested bovine cartilage in diluted bovine calf
16 serum. Under a non-migrating contact, the friction force increased and hence shear force applied to
17 the opposing articular cartilage also increased, resulting in minor damage to the cartilage surface.
18 This worse case testing scenario was used to discriminate between material formulations and
19 revealed the increase in friction and damaged area was lowest for the hybrid containing the most
20 silica. Further friction and wear tests on one hybrid formulation with an elastic modulus closest to
21 that of cartilage were then conducted in a custom incubator system. This demonstrated that over a
22 five day period the friction force, cell viability and glucosaminoglycan (GAG) release into the
23 lubricant were similar between a cartilage-cartilage interface and the hybrid-cartilage interface,
24 supporting the use of these materials for cartilage repair. These results demonstrate how tribology
25 testing can play a part in the development of new materials for chondral tissue engineering.

26

27 Statement of Significance

28 Designing materials that maintain the low friction and wear of articular cartilage whilst supporting
29 the growth of new tissue is critical if further damage is to be avoided during repair of cartilage
30 defects. This work examines the tribological performance of a SiO₂/PTHF/PCL-diCOOH hybrid
31 material and demonstrates a testing protocol that could be applied to any proposed material for
32 cartilage regeneration. Tribological tests demonstrated that changing the hybrid composition
33 decreased friction and reduced damage to the cartilage counterface. This study demonstrates how
34 tribological testing can be integrated into the design process to produce materials with a higher
35 chance of clinical success.

36

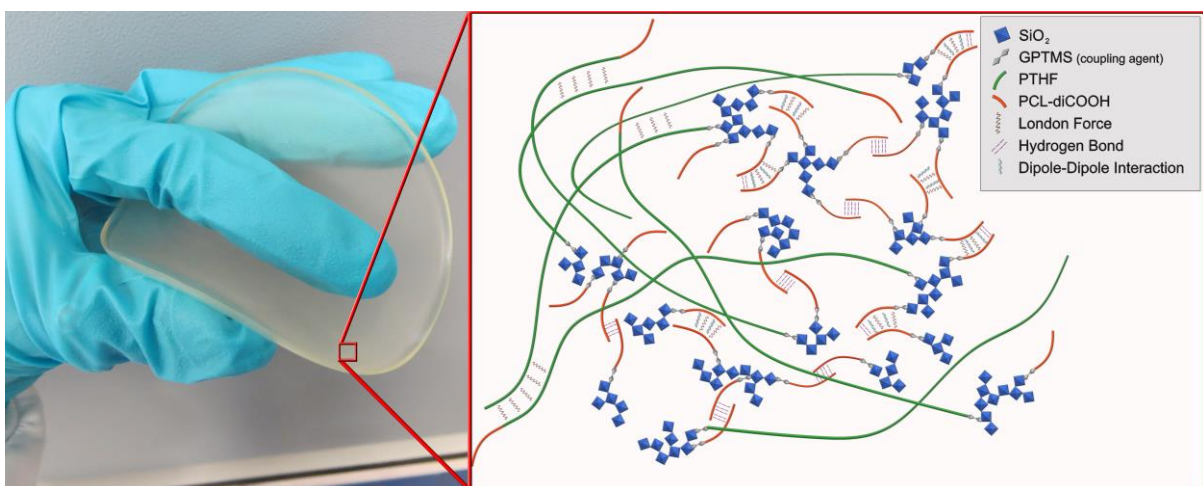
37 1. Introduction

38 The regeneration of cartilage in osteochondral defects remains a challenge. Clinical treatments like
39 Autologous Chondrocyte Implantation and microfracture often regenerate fibrocartilage rather than
40 the desired hyaline cartilage. Scaffolds used in tissue engineering aim to solve this problem by
41 providing the right conditions for hyaline cartilage to form. Such scaffolds must integrate with both
42 the native cartilage and the underlying subchondral bone, retain their structural integrity long
43 enough for cartilage to reform and not cause any damage to the opposing cartilage tissue [1]. An
44 ideal device would stimulate regeneration of articular cartilage while also providing a surface that
45 preserves the integrity of the opposing surface and also transmit load to the regenerating tissue
46 before safely biodegrading. Current scaffold materials have been proposed, but biodegradable
47 devices with a combination of suitable mechanical properties and integration of these materials with
48 the surrounding healthy cartilage are yet to be developed [2].

49 Bioactive glasses bond with both hard [3] and soft tissues [4], but they are stiff, hard and brittle,
50 making them unsuitable for implanting into the articulating surface, even as composites, as the
51 particulates could cause wear [5]. Incorporating ceramics or glasses into polymer composite
52 materials can lower stiffness, but composites often suffer from the polymer masking the bioactive

53 phase; a mismatch in the rate of biodegradation of the components and a lack of bonding between
54 the components, which lowers the mechanical strength from the theoretical values [6]. To overcome
55 these deficiencies, inorganic/organic hybrid materials have been developed. In Class II and Class IV
56 hybrid materials, the inorganic glasses and organic polymers are nanoscale co-networks with
57 covalent bonds (coupling) between the networks [7]. Mechanical strength and degradation rate can
58 be adjusted to the desired values for a particular application by changing the ratio of inorganic to
59 organic and amount of covalent coupling in the hybrid.

60 Tallia *et al.* recently presented the development of a novel hybrid based on silica (SiO_2), carboxylated
61 poly(ϵ -caprolactone) (PCL-diCOOH) and poly(tetrahydrofuran) (PTHF) [8], as illustrated in Figure 1.
62 The transparency (Figure 1), and TEM images in previous work, indicated that the material had a
63 homogenous microstructure. By controlling the weight percent (wt%) of SiO_2 in the final material,
64 the storage modulus in tension, E' , varied between 0.4-132 MPa [8] covering the reported range of
65 moduli for articular cartilage [9]. When 3D printed into a scaffold with a grid-like structure of ~ 250
66 μm wide pore channels, the scaffold stimulated chondrocytes to produce matrix representative of
67 articular cartilage matrix and provoked human mesenchymal stem cells (MSCs) down a
68 chondrogenic path, when cultured with chondrogenic media [8].



69
70 **Figure 1. The transparent appearance of cast SiO_2 /PTHF/PCL-diCOOH hybrid material with a**
71 **schematic of the structure of the hybrid.**

72 Although the characteristics of this material are promising in terms of cell regeneration and
73 mechanical stiffness, the tribological properties have not yet been established. The material itself
74 must be able to withstand damage under sliding or it will not survive long enough to support the
75 new tissue growth. We will also compare the hybrid material to PCL alone, as it is a popular polymer
76 for cartilage repair strategies, but can surface damage under shear [10]. Here, we investigate the
77 tribological properties of the hybrid biomaterial for the first time, as a function of composition, and
78 determine whether release of the biodegradable polymer from the hybrid affects wear. Importantly,
79 we investigate the tribological properties of the hybrid sliding against “living” cartilage if damage to
80 the healthy cartilage during defect repair, as seen previously [11, 12], is to be avoided.

81 Most *in vitro* testing of cartilage against implant materials has previously been short term, typically
82 less than 24 hours, as the properties of the cartilage tissue begin to degrade with time. Often, in
83 short term testing, a cartilage pin is loaded in such a way as to give a non-migrating contact, which
84 reduces the fluid in the tissue and results in higher friction forces and increased wear [13]. A non-
85 migrating contact is where the cartilage sample is loaded constantly throughout the test and thus
86 the intrinsic fluid-load support mechanism is suppressed

87 . This testing configuration has been used to test chondroplasty and hemiarthroplasty materials [14-
88 16] and although more likely to result in cartilage damage, it allows for greater discrimination
89 between the effects of experimental variables [17].

90 Recent advances in cell culture techniques and bioreactor design mean it is now possible to consider
91 longer term testing of cartilage tissue in a more physiological setup, bridging the gap between *in*
92 *vitro* testing and animal studies [18]. Wimmer *et al.* developed a cartilage bioreactor that
93 approximates the rolling-sliding kinetics of a knee joint which can be housed in an incubator [19, 20].
94 We made a single-station system, based on their design, with some modifications to allow friction
95 measurements to be made during testing.

96 Here, five SiO₂/PTHF/PCL-diCOOH hybrid materials containing increasing wt% SiO₂ were investigated
97 to determine their suitability as potential materials for cartilage regeneration, particularly as to
98 whether they could take the role of articulating surface, in terms of friction and wear resistance.
99 From these formulations, one material was taken forward for testing against cartilage explants
100 maintained in cell culture conditions. This work will inform the continuing material design process to
101 determine the best hybrid formulation for articular cartilage repair.

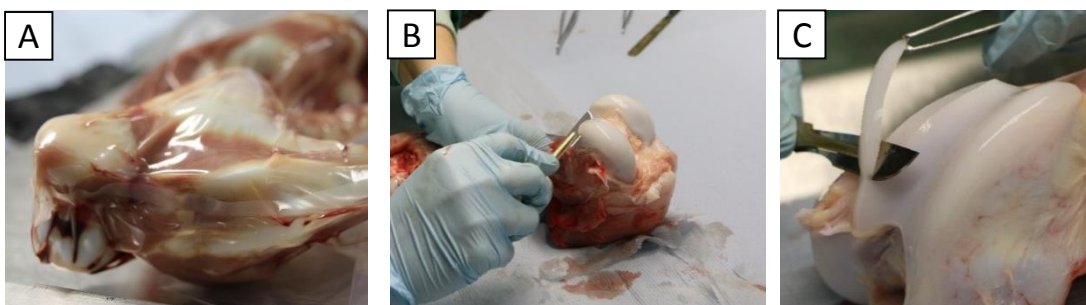
102

103 2. Materials and methods

104 2.1 Materials

105 SiO₂/PTHF/PCL-diCOOH hybrid materials were prepared in a two-step procedure, as described in
106 Tallia *et al.* [8]. First, TEMPO oxidation was applied to PCL-diol (average M_n = 530 Da), producing the
107 dicarboxylic acid form (PCL-diCOOH), that was then introduced into the following sol-gel hybrid
108 synthesis. An organic precursor solution of the PCL-diCOOH (1 mol), (3-
109 glycidyloxypropyl)trimethoxysilane (GPTMS, 2 mol) and boron trifluoride diethyletherate (BF₃·OEt₂,
110 0.5 mol) was prepared in THF and stirred at room temperature for 1.5 hours, during which
111 polymerisation of THF to pTHF occurred. At the same time, tetraethyl orthosilicate (TEOS), the silica
112 precursor, was completely hydrolysed in a stoichiometric volume of deionised water by 1 M
113 hydrochloric acid, at a ratio of 1:3 % v/v with respect to water. When the two separate solutions
114 were fully reacted, the TEOS hydrolysis solution was added dropwise to the organic precursor
115 solution and stirred at room temperature for 30 minutes to form the hybrid sol, that was cast in
116 cylindrical polytetrafluoroethylene (PTFE) containers (internal Ø = 130 mm), which were placed at
117 40°C for ageing and drying. After drying, the shrinkage inherent in the sol-gel process determined
118 the final dimensions of the samples in the shape of thin discs. Five different TEOS/PCL-diCOOH
119 %w/w (0/100, 60/40, 70/30, 80/20, 90/10) were used in order to prepare the five hybrid
120 compositions tested. All chemicals were purchased from Sigma-Aldrich and VWR, UK, unless

121 specified otherwise. At the end of the drying step, the SiO₂ content of the hybrid was determined by
122 thermogravimetric analysis (TGA). The composition of the five formulations tested is given in Table
123 1. For all materials, the free surface (not in contact with the mould during casting) was tested.
124 For short term friction tests, cartilage pins of 8 mm diameter removed from the femoral condyle of
125 an adult sheep using a biopsy punch and stored at -20°C in phosphate buffered saline (PBS). Before
126 use, samples were defrosted overnight and then secured in an aluminium holder using bone cement.
127 For bioreactor testing, a similar protocol as described previously was followed [19]. Cartilage
128 samples were removed from stifle joints of bovine calves obtained from a local abattoir within 48
129 hours of slaughter (Figure 2A). The joints were kept intact until dissection, at which time cartilage
130 was removed from the medial and lateral femoral condyles (Figure 2B) and the rim of the trochlear
131 groove using a scalpel (Figure 2C). Removed cartilage was stored in sterile PBS supplemented with
132 100 µg mL⁻¹ streptomycin and 100 µg mL⁻¹ penicillin (Figure 2D). Cartilage flats were prepared from
133 the femoral condyle cartilage using a custom oval punch to give samples with length 20 mm and
134 width 14 mm (Figure 2E). These were placed in sterile petri dishes and held in position by porous
135 polyethylene (PE) wafers under semi-confined compression (Figure 2F). The resulting samples had a
136 convex curvature with a typical radius 20 mm along the long axis of the sample. At the same time
137 SiO₂/PTHF/PCL-diCOOH hybrid samples were cut using the same oval punch and secured using
138 double sided tape on a PE wafer and secured in sterile petri dishes. Cartilage balls were prepared by
139 taking the cartilage from the rim of the trochlear groove and cutting into strips 8 mm wide by 20 mm
140 long. These were secured to poly(oxymethylene) copolymer (POM-C) balls using polyamide-6
141 sutures (Figure 2G).



147
148
149
150
151
152
153
154
155
156
157
158
159
160
161
162
163
164
165
166
167
168
169
170
171
172
173

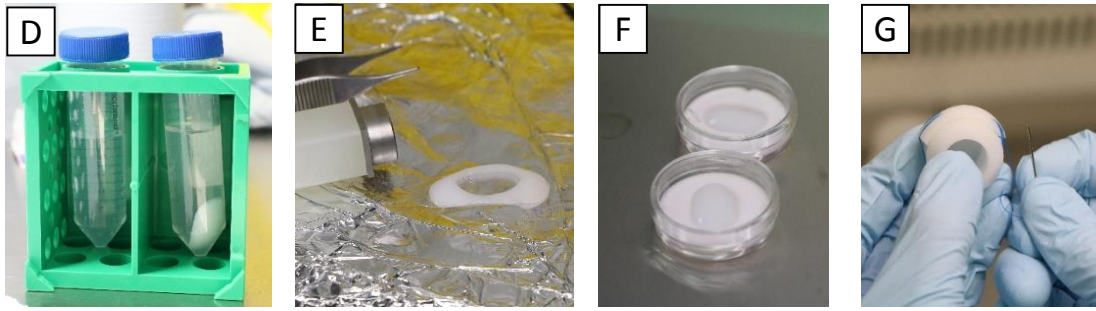


Figure 2 Retrieval and preparation of cartilage samples: (A) joints as received; (B) removing cartilage from femoral condyles; (C) removing cartilage from rim of trochlear groove; (D) storage in PBS supplemented with antibiotics; (E) removal of cartilage flat with custom punch; (F) samples confined in petri dishes; (G) samples secured on POM-C ball using surgical sutures.

Cartilage and hybrid samples were cultured at 37 °C and 5% CO₂ in culture media composed of DMEM (4.5 g L⁻¹ glucose; Invitrogen) supplemented with 10% (v/v) fetal bovine serum, 100 µg mL⁻¹ streptomycin, 100 µg mL⁻¹ penicillin, and 50 µg mL⁻¹ L-ascorbic acid. Media was changed daily. Samples were cultured for 24 hours before testing began.

2.2 Contact angle measurements

Static contact angles were determined using the sessile drop technique using pure water. A 5 µl drop was placed gently on the surface of the hybrid material and photographed. The shape of the drop was fitted using a sessile drop model (Krüss Surface Science, Hamburg, Germany). For each hybrid formulation measurements were taken in five different areas and averaged.

2.3 Atomic Force Microscopy measurements

Atomic Force Microscopy (AFM, Alpha 300 RA, WITec, Ulm, Germany) images were acquired at a scan rate of 1 Hz in contact mode. A silicon nitride tip with a nominal cantilever spring constant of 0.2 N/m (XVA3000, LOT-Quantum Design Ltd, Surrey, UK) was used.

174 2.4 Short term friction and wear tests

175 Short term friction and wear tests were carried out of all five hybrid compositions, in a monolithic
176 form, in order to choose the best composition that would go forward for bioreactor testing.

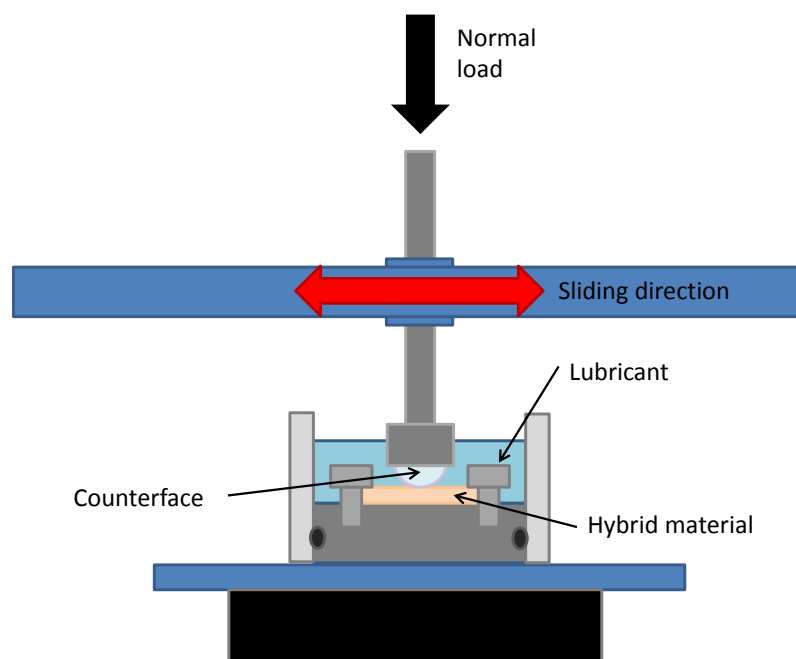
177

178 2.4.1 Friction measurements

179 A custom tribometer was used to conduct friction tests under linear reciprocating motion (Figure 3).

180 Hybrid material samples were clamped on a stainless steel holder. Cartilage pins were reciprocated
181 with a stroke length of 5 mm at 1 Hz, giving an average speed of 10 mm s⁻¹ for 1 hour. Tests were
182 conducted in bovine calf serum (BCS) diluted to 20 g L⁻¹ protein in distilled water. Cartilage flats and
183 polished CoCrMo (ISO 5832-12) disks were used as positive and negative controls respectively.

184 CoCrMo was chosen as a negative control as this is the material from which a medical device in
185 current clinical use for partial resurfacing is made [21]. Tests were conducted at room temperature
186 (20°C) with six repeats performed for each set of conditions. Normal loads and friction forces were
187 measured by a 6-axis load cell (Gamma, ATI Industrial Automation, USA).



188

189 **Figure 3 Schematic of custom tribometer used to measure friction.**

190

191 All tests were conducted under a deadweight load of 1 N. Fuji pressure sensitive film (ultra-super
192 low grade, Fuji Photo Film Co., Japan) was used to measure the contact area and the average contact
193 pressure calculated for a deadweight load of 1 N. Contact pressures are given in Table 1 along with
194 calculated compressive moduli for the hybrid material based on Hertzian contact theory (see
195 supplementary material S1).

196

197 2.4.2 Wear measurements

198 Following testing, samples were rinsed with deionised water, gently cleaned with 2 % detergent
199 solution and examined under an optical microscope for signs of surface damage. Macroscale wear
200 was investigated using a NT9100 Veeco white light interferometer (WLI) with a magnification of 11x.
201 Surface roughness, R_a , was calculated over an area of 430 μm x 547 μm . WLI was used rather than
202 AFM as the wear track area was in the order of mm^2 .

203

204 2.5 Bioreactor tests

205 From the short term tests, the hybrid with 25 wt% silica content was tested in a bioreactor test,
206 which involved using rigs, such as that shown in Figure 3, inside a cell culture incubator at 37 °C with
207 an atmosphere of 5% CO_2 .

208

209 2.5.1 Friction measurements

210 Before testing, the culture media, in the petri dishes containing cartilage, was exchanged for fresh
211 media. Petri dishes containing the cartilage or hybrid flat samples (Figure 2F) were fixed to a 6-axis
212 load cell allowing simultaneous measurement of normal and horizontal forces. Cartilage balls (Figure

213 2G) were press fit onto a stainless steel shaft on a translation and rotation stage. A 10 N load was
214 applied as a deadweight. In the bioreactor tests, contact pressures were not directly measured but
215 can be calculated from Hertzian contact theory to be approximately 0.2 MPa for a cartilage-cartilage
216 pairing, and 0.1 MPa for a cartilage-hybrid pairing. The cartilage ball was reciprocated with a
217 translation of 10 mm combined with a rotation of 45° to give a rolling motion in which the point of
218 contact would move on both cartilage surfaces (i.e. a migrating contact configuration in contrast to
219 the non-migrating contact described in Section 2.4.1). Motion was applied at 0.5 Hz for 1 hour after
220 which the test media was collected, fresh media added and the samples returned to the incubator.
221 For each sample, 1 hour tests were performed on five sequential days. Four cartilage-cartilage and
222 four hybrid-cartilage pairs were tested.

223

224 2.5.2 Cell Viability

225 Cell viability within the cartilage was assessed with a LIVE/DEAD cell assay (Invitrogen) according to
226 the manufacturer's protocol. After the testing period, cartilage samples were removed from their
227 holders and rinsed in sterile PBS. They were then bisected perpendicular to the reciprocating
228 direction and thin slices were obtained using a scalpel and placed in 12 well plates. The tissues were
229 incubated with 2 µM calcein AM and 4 µM ethidium homodimer-1 in sterile PBS, staining live cells
230 with green fluorescence and dead cells with red fluorescence. After 40 min, chondrocytes were
231 imaged using an epifluorescence microscope (Axio Observer, Zeiss) using 5x and 10x objectives.

232

233 2.5.3 Glycosaminoglycan release into media

234 Media from friction tests was collected and stored at -20°C. For analysis, 0.5 mL media was mixed
235 with 0.5 mL papain digestion buffer (5 mM L-cysteine, 5 mM EDTA, pH 8.0 containing 125 mg mL⁻¹
236 papain) overnight at 65°C. The dimethylmethylene blue (DMMB) dye reaction was used to quantify

237 glycosaminoglycans (GAGs) released into solution. 200 μL of digested media was added to 2 mL of
238 DMMB reagent solution (40 mM NaCl; 40 mM glycine; 46 mM DMMB, 10 mM acetic acid, pH 3.0),
239 mixed for 30 seconds and the absorbance read at 525 nm using UV-Vis spectrometer (Perkin-Elmer,
240 UK). A calibration curve was compiled using shark cartilage chondroitin sulphate solutions with
241 concentrations between 10 and 50 $\mu\text{g mL}^{-1}$. Calibration solutions were prepared in culture media
242 and also digested with papain.

243

244 2.5.4. Hybrid wear measurements

245 As before, samples were rinsed with deionised water, gently cleaned with 2 % detergent solution
246 and examined under an optical microscope before measurement of surface roughness using WLI.

247 Release of Si into the testing media was assessed using inductively coupled plasma – optical
248 emission spectrometer (Thermo Scientific iCAP 6300 Duo ICP–OES) with a sensitivity of 1 ppb.

249 Solutions were prepared by filtration of the media to 0.2 μm (Corning® syringe filters) and dilution
250 by factor 2 in deionised water. Si concentration was measured in the radial direction of the flame
251 and calibration with standards 0, 0.1, 0.2, 0.4, 0.8, 1, 2, 5, 10 $\mu\text{g mL}^{-1}$ was carried out at the
252 beginning of the sequence. The relative polymer content of the hybrid was assessed at day 5 by
253 thermogravimetric analysis (TGA) at a heating rate of 10 K min^{-1} to 800°C and compared with non-
254 loaded soaked samples.

255

256 2.6 Statistical analysis

257 Mean values are reported for all tests. Statistical analysis was performed using a one-way analysis of
258 variance (ANOVA) using the software package SPSS. A posthoc Tukey test with statistical significance
259 evaluated at $p < 0.05$ was used as a comparison of means.

260

261 3. Results

262 3.1 Material characterisation

263 Contact angle measurements showed that at low silica content, samples were hydrophilic. As the
264 wt% silica increased the samples became progressively more hydrophobic and the contact angle
265 increased from $56 \pm 3^\circ$ for the 3 wt% silica to $94 \pm 2^\circ$ for the 39 wt% silica (Figure 4). This is in
266 contrast to expectations as the pure silica is extremely hydrophilic and so it was expected that with
267 increasing silica the hybrid material would also become more hydrophilic. It has previously been
268 shown that the surface hydrophobicity of cast dry PCL films is determined by the solvent
269 environment during drying [22], which may explain this unexpected result. Hybrid materials with a
270 higher SiO₂ content are formed with more TEOS. This in turn increases the concentration of solvent
271 in the cast drying atmosphere which may attract more of the hydrophobic segments of the PCL
272 molecules to the surface.

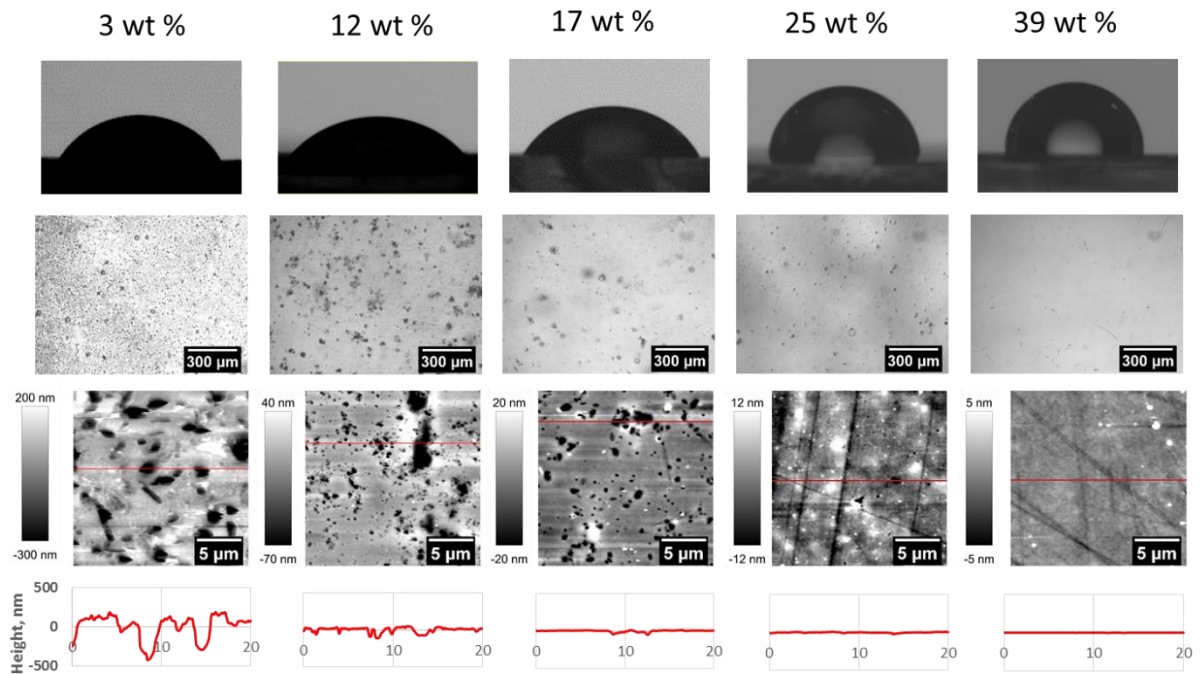
273 **Table 1. Hybrid formulations and properties. Actual wt% inorganic was determined previously [8].**

Ratio by mass of TEOS:PCL-diCOOH	Actual wt% Inorganic	Calculated average contact pressure with cartilage pin, MPa (\pm S.D.)	Calculated range of compressive modulus, MPa
0:100	3	0.021 ± 0.002	0.09-0.14
60:40	12	0.032 ± 0.001	0.19-0.30
70:30	17	0.039 ± 0.006	0.22-0.45
80:20	25	0.071 ± 0.006	0.63-1.28
90:10	39	0.446 ± 0.102	2.12-208

274

275 The free surface of the 5 formulations was examined by optical microscopy and AFM. At low SiO₂
276 content, the hybrids had a significant number of surface features contributing to a high surface
277 roughness. AFM images (Figure 4) revealed these features to be holes in the hybrid material. This
278 could influence the contact angle. At low SiO₂ content, both the number of holes and the average
279 size of the holes were larger (detected in the roughness data, Figure 5B). The holes are consistent
280 with pockets of solvent that became trapped during the cast-drying process. For the high wt % SiO₂

281 hybrids, the drying process was longer, so the solvent is less likely to be trapped resulting in a
 282 smoother surface [23]. The behaviour of polymer and silica during drying may also play a role, with
 283 the polymer giving a more irregular surface, whereas the silica tends to give very smooth surfaces.



284
 285 **Figure 4. First row: Contact angle measurements; Second row: Optical Microscope images of**
 286 **surface features of the hybrid; Third row: AFM images (20 μm x 20 μm) showing that the surface**
 287 **features to be small pits on hybrid surface; Bottom row: height profile across cross-section of AFM**
 288 **images, showing typical depth of pits and general surface roughness.**

289
 290 3.2 Short term testing results

291 3.2.1 Friction results

292 Figure 5A shows the friction coefficient for cartilage against the hybrid materials at 5 seconds and
 293 3500 seconds and against negative and positive controls. **Full friction traces for all tests are included**
 294 **in Supplementary Material S2.** In these tests, the cartilage pin experienced a non-migrating contact,
 295 meaning there was no opportunity for fluid replenishment into the cartilage during the test. Thus,
 296 the interstitial fluid in the cartilage flowed out of the contact area, resulting in less fluid load support
 297 and increased solid-solid contact. This in turn led to a rise in the friction coefficient with time [16].

298 After 5 seconds, there was no statistically significant difference in the measured friction coefficient
299 between the positive cartilage-cartilage control and any of the hybrid materials against the cartilage,
300 or the negative CoCrMo control against the cartilage ($p=0.178$). At $t=5$ seconds, the cartilage was still
301 hydrated and the friction coefficient was at its lowest. This is representative of the conditions in a
302 healthy joint.

303 After 1 hour, the cartilage in contact lost its interstitial fluid resulting in a worst-case friction
304 coefficient. Therefore, after 1 hour, the coefficient of friction for all hybrid materials and the positive
305 control increased, and the friction coefficient increased as SiO_2 content in the composition
306 decreased. This increase was lowest for 39 wt% SiO_2 sample, which reached an average friction
307 coefficient of 0.17. This increase was less than that observed for the CoCrMo control, but greater
308 than the cartilage/cartilage control at 1 hour.

309

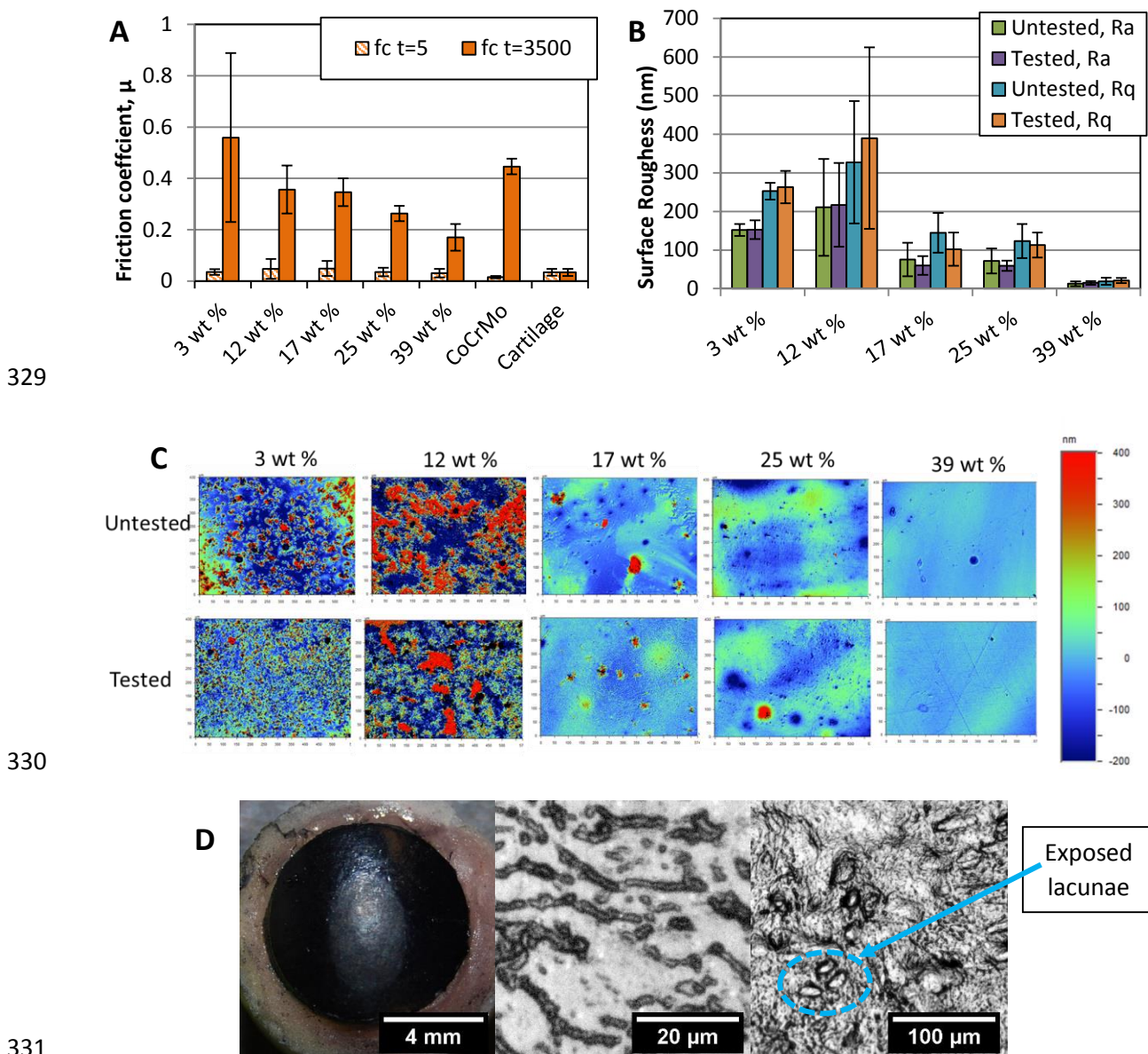
310 3.2.2 Wear

311 For all hybrid formulations, typical surface maps and the average surface roughness, measured by
312 WLI, as received and after all tests, are shown in Figure 5 B,C. The surface maps show that the
313 surface roughness was highest for hybrids with low silica content and decreased as silica content
314 increased, which was consistent with the AFM scans (Figure 4).

315 For each hybrid, the average surface roughness after testing was compared to the surface roughness
316 in the as received condition using a one-way ANOVA with significance of 0.05. This showed there
317 was no statistically significant change in surface roughness. This is visually demonstrated in the
318 surface maps which show no discernible change in the morphology after testing.

319 Although no wear was observed on the hybrid samples, the cartilage pins had surface damage that
320 was observable under the optical microscope. This damage was limited in area so that a boundary
321 between damaged and undamaged cartilage was visible in most cases. Optical images of the surface

322 damage at higher magnification showed the formation of fibrous structures or rolls as well as
 323 exposed cartilage lacunae (Figure 5D). This indicates that there was disruption to the surface
 324 amorphous layer which is the uppermost layer of cartilage formed of a mixture of proteins, lipids
 325 and glycosaminoglycans [24, 25]. Surface area measurements of the damaged region, taken using
 326 Image J, showed the extent of this damaged region decreased as silica content increased from 12.8
 327 mm² for 2.5 wt% SiO₂ to 5.2 mm² for 39 wt% SiO₂. This is despite the lower contact pressure for the
 328 softer hybrids with a lower wt% SiO₂ content.



332 **Figure 5. Friction and wear results for short term tests for cartilage pins against the hybrid**
 333 **materials of different wt% of inorganic component: (A) friction coefficient at t = 5 s and t = 3500 s**

334 for cartilage pins lubricated by bovine serum against hybrids with different wt% of inorganic
335 components, a CoCrMo disk (negative control) and a cartilage flat (positive control); (B) average
336 surface roughness (R_a) and root mean square roughness (R_q), measured by WLI, showing no
337 change before and after friction tests; (C) typical WLI height maps of hybrid materials, showing
338 variation with wt% of inorganic components; (D) optical microscope images of a cartilage plug
339 showing a worn area; increasing magnification showed line or rolled features (middle) and
340 exposed lacunae where chondrocytes would be situated (right).

341

342 3.3 Bioreactor test results

343 3.3.1 Friction measurements

344 For each testing pair (cartilage against cartilage or 25 wt% SiO₂ hybrid against cartilage), the friction
345 coefficient at the end of 1 hour of testing was calculated as the average of the last 5 cycles (Figure
346 6A). The measured friction for each pair stayed consistent over five days (with the exception of the
347 third hybrid-cartilage pair on day 4 which was due to a set-up error where the ball came loose on the
348 supporting shaft and so no friction data is shown for this day), even though there was some variation
349 between testing pairs. This variation is typical of tissue tests where the exact geometry and tissue
350 properties change from sample to sample. The average friction coefficient for the four cartilage-
351 cartilage pairs was 0.013 ± 0.008 , which was statistically significantly different to the average
352 friction for the hybrid-cartilage pairs of 0.005 ± 0.002 ($p < 0.001$). The friction trace for the 8 sample
353 pairs over the whole 1 hour duration is included in Supplementary Material S3.

354

355 3.3.2 Cell viability

356 For cartilage-cartilage pairs, an image of the entire cross section of the flat side was captured by
357 combining several images at 5x magnification. This whole cross section image demonstrated that
358 there was good cell viability through the depth of the cartilage seven days after harvest (Figure 6B).
359 Regions of dead cells were observed at the edges of the cross section at the interface with the PE
360 wafer. There was no sign of increased cell death in the area of articulation.

361 On the cartilage balls, a clear area of dead cells was seen in the loaded surface region. This region
362 varied in thickness but extended to an average depth of 0.4 mm below the surface. Cell viability was
363 measured for a sample area of 0.25 mm² in the loaded region. The average cell viability in this area
364 was 29 ± 9 % and 34 ± 13 % for cartilage-cartilage and hybrid-cartilage pairs respectively showing no
365 statistically significant difference ($p=0.527$), Figure 6C.

366

367 3.3.3 GAG release into media

368 For cartilage-cartilage testing pairs there are two possible sources of GAG release (the cartilage ball
369 and cartilage flat) whilst the hybrid system only has one cartilage surface, the cartilage flat. To
370 compare GAG release between the systems, it was assumed that the cartilage ball and flat would
371 equally contribute to GAG release and so this measurement was divided by 2. The average GAG
372 release into the test media over five days was between 7-18 µg mL⁻¹ per day (Figure 6D), with larger
373 variations in GAG release for cartilage-cartilage pairs. The average release over all five days for the
374 cartilage-cartilage group was 13.6 ± 4.84 µg mL⁻¹ which was slightly higher than the 8.0 ± 2.8 µg mL⁻¹
375 measured for the cartilage-hybrid testing groups. A one-way ANOVA shows the reduction to be
376 statistically significant with $p < 0.001$.

377

378

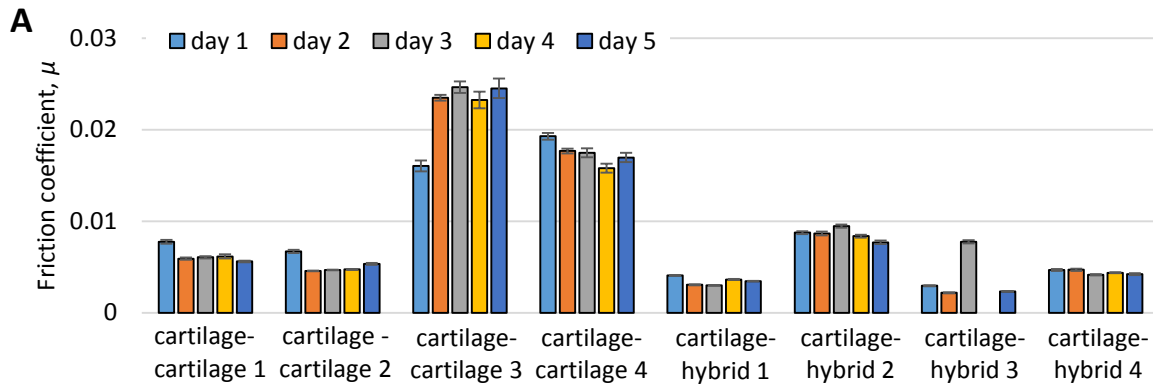
379

380

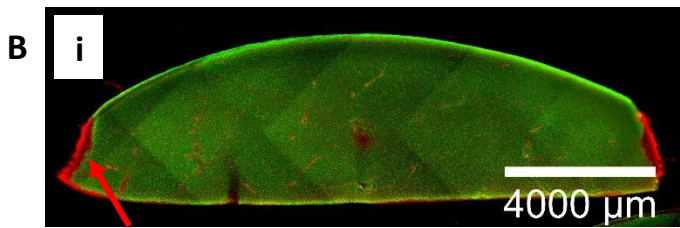
381

382

383

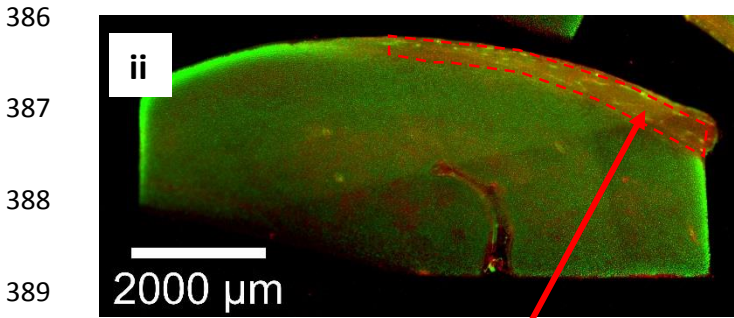


384



Dead cells at interface with PE wafer

385



Dead cells in articulating region of cartilage ball

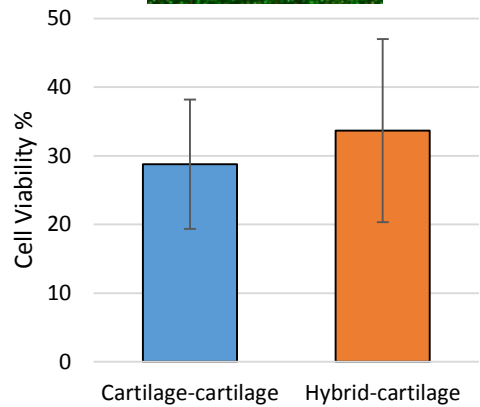
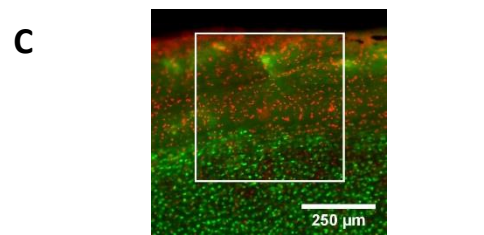
386

387

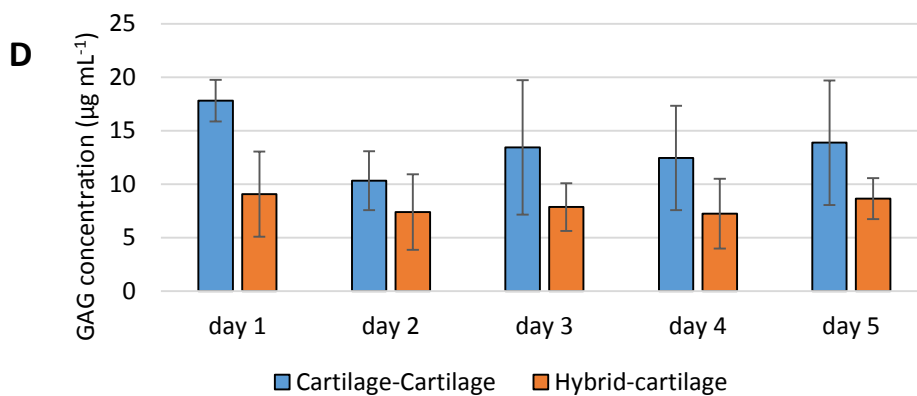
388

389

390



391



392

393

394

395

396

397 **Figure 6 Friction and wear results for bioreactor tests of cartilage against cartilage and 25 wt% SiO₂**

398 **hybrid against cartilage: (A) friction coefficient for each testing pair at end of 1 hour of testing,**

399 **daily; (B) stitched fluorescence images showing LIVE/DEAD stain across the cross section of (i) a**

400 **cartilage flat (ii) a cartilage ball; (C) typical sampling region to assess cell viability and average**

401 results for testing combinations; (D) average GAG release into test media over 5 testing days as
402 measured by DMMB assay, normalised to number of cartilage surfaces.

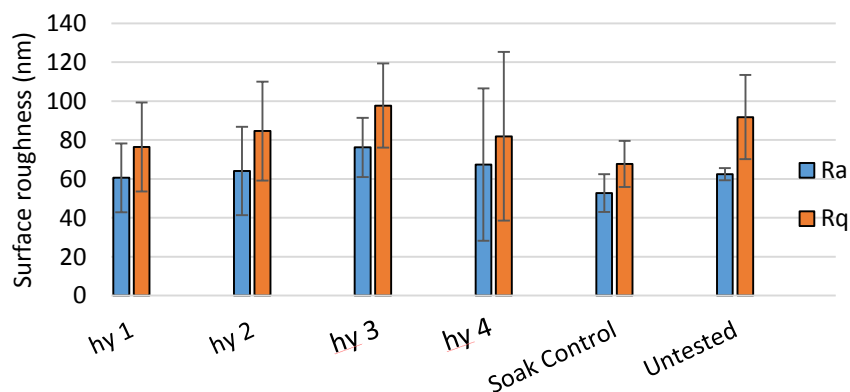
403

404 3.3.4 Hybrid wear measurements

405 Following testing, the hybrid samples were examined under an optical microscope and no signs of
406 wear were observed. WLI measurements found that the average surface roughness (R_a) and root
407 mean square roughness (R_q) of the tested hybrid varied between 52-76 nm and 68-98 nm but were
408 not significantly different to the untested control (as prepared unloaded hybrid, Figure 7). The values
409 were also similar for the hybrid that was soaked in the media but not friction tested ($p=0.311$ and
410 $p=0.298$ respectively).

411 From TGA measurements, the initial organic content of the hybrid of 82.9 wt% was reduced by
412 soaking (with no loading) by $\delta_{\text{soaking}} = -1.2$ wt% compared to the loaded samples which show an
413 average additional loss of polymer due to wear of $\delta_{\text{wear}} = -0.2$ wt%. ICP-OES measurements show a
414 small peak of Si release of $2.3 \pm 0.4 \mu\text{g mL}^{-1}$ at day 1, reducing to below $1 \mu\text{g mL}^{-1}$ after day 4.

415



416

417 **Figure 7. Average Surface Roughness (R_a) and root mean square roughness (R_q) of the hybrid**
418 **materials, measured by WLIF, showing no change before (Untested) and after friction tests (hy1-**
419 **4). Hybrid materials that were soaked in the media but not loaded (Soak control) were also tested.**

420

421 4. Discussion

422 This is the first study to investigate the tribology of silica/polymer hybrid materials designed for
423 chondral repair applications. Increasing the silica content of the hybrid material improved both the
424 friction and wear performance (Figure 5) and when tested against cartilage in a bioreactor, the
425 hybrid formulation with 25 wt% SiO₂ had similar performance to a cartilage-cartilage pair in terms of
426 friction forces, cell viability and cartilage wear (Figure 6). There were no surface changes in the
427 hybrid material, indicating little wear (Figure 7). The amount of polymer released from the hybrid
428 material was not increased due to friction testing. This evidence is supportive of further
429 development of the hybrid material for chondral repair applications.

430 The five formulations of hybrid materials tested had different surface properties in terms of
431 hydrophobicity (Figure 4) and surface roughness (Figure 5), both of which can impact the friction
432 performance of a material. Some proteins when adsorbed on hydrophobic surfaces can increase
433 friction forces [26, 27], whilst for the nanoscale roughness seen here other polymers have shown an
434 increase in friction with higher roughness [28, 29]. As an increase in SiO₂ content increased
435 hydrophobicity (Figure 4) but reduced surface roughness (Figure 5). These changes oppose each
436 other and it is only possible to determine the relative effects through friction testing, which showed
437 increasing SiO₂ content improved the overall results (Figure 6).

438 AFM showed the presence of holes in the hybrid surface (Figure 5), causing roughness, which were
439 more frequent at higher solvent evaporation rates, i.e. at lower silica contents [25]. By controlling
440 the solvent evaporation process more closely, formation of the holes could be reduced, potentially
441 improving the friction performance of materials with a lower SiO₂ content. Removal of these holes
442 which act as stress concentrations would also reduce the likelihood of crack formation in the
443 material. However, at our chosen composition of 25 wt% silica, the holes were low in number.

444 For materials that articulate against cartilage, low friction prevents high shear strains and stresses in
445 the cartilage which can lead to chondrocyte death and collagen cleavage [30]. In our test that was

446 most representative of the *in vivo* situation (moving surfaces in media), at $t = 5$ s there was no
447 statistical difference between the friction coefficient for cartilage-cartilage contact or cartilage-
448 hybrid contact for any formulation (Figure 5A). However, as fluid was lost from the cartilage, the
449 friction force increased as significant wear of the cartilage surface was generated.

450 For the testing configuration that was a worst-case scenario [17] (cartilage pins), wear was observed
451 on the cartilage pin when it had made contact with the hybrid material (Figure 5). The wear
452 observed was more severe than would be expected in practice, but the test allowed discrimination
453 between test variables and allowed us to choose the hybrid formulation to test in the bioreactor (25
454 wt% SiO₂). Optical images of the worn area showed a disruption of the continuous surface
455 amorphous layer of the cartilage and exposure of lacunae. The size of the worn area decreased as
456 SiO₂ content in the hybrid increased, which may be explained by an increase in compressive stiffness
457 of the hybrid. Whilst this agrees with the friction results indicating increasing SiO₂ content is
458 beneficial this must be balanced against the risk of increasing contact pressures which can also be
459 detrimental to tissue health.

460 For bioreactor testing, the 25 wt% formulation was chosen as this had a high SiO₂ content, giving
461 good friction and wear properties but also had a compressive modulus closest to cartilage. In
462 agreement with the short-term tests, the coefficient of friction of the hybrid-cartilage couple was on
463 average lower than a cartilage-cartilage pair when tissue fluid levels were maintained (Figure 6). This
464 is most likely due to the more regular geometry of the hybrid samples rather than an improvement
465 on the frictional performance of cartilage. The hybrid samples are manufactured so have a
466 repeatable, flat geometry. The cartilage samples are retrieved and as mentioned in section 2.1
467 cartilage flats had a convex curvature with a typical radius of 20mm. This curvature will have some
468 effect on the measured tangential forces during sliding, and so will cause greater variation between
469 test pairs in the calculated friction coefficient. Healthy cartilage lubricated with synovial fluid is
470 expected to see a shear strain of approximately 0.02-0.05 based on a coefficient of friction of 0.01

471 [31]. In the bioreactor, friction coefficients between 0.005 and 0.025 were measured for testing
472 pairs. This gives a maximum lateral force of 0.25 N, which if we assume to act over the cross-
473 sectional area of the sample (5 mm x 14 mm) the maximum shear stress was approximately 3.6 kPa.
474 Assuming a cartilage shear modulus, G , of 0.26 MPa [31], maximum shear strains can be estimated
475 to be 0.014, which is in the range that healthy tissue is exposed to and so not expected to cause
476 tissue damage. This is consistent with our LIVE/DEAD assay of the “flat” cartilage specimens, but not
477 consistent with the observed cell death seen in the articulating region for the cartilage balls. The
478 difference in cell viability may be due to the source location of the cartilage: for the cartilage balls,
479 the cartilage was taken from the rim of the trochlear groove, which is not usually subjected to high
480 loads during motion, whereas the cartilage flats were taken from the femoral condyles which do
481 experience loading during gait. This is a factor to consider in further experiments of this type.
482 Although cell viability was reduced on the articulating surface of the ball, subsurface viability did not
483 change, nor did the viability of the surface within 500 μm of the articulating surface for the cartilage-
484 cartilage or the hybrid-cartilage pair, indicating that it was not caused by the properties of the hybrid
485 material.

486 The release of GAG from cartilage tissue is associated with cartilage degeneration and may indicate
487 early wear of samples. The concentrations of GAG measured here were around $10 \mu\text{g mL}^{-1}$ for a one
488 hour period, which is similar in magnitude to the $60 \mu\text{g mL}^{-1}$ for three hours reported by Trevino *et*
489 *al.* [19]. The amount of GAG released was actually lower for the cartilage-hybrid tests than it was for
490 the cartilage-cartilage pairs, even when adjusted for the number of cartilage surfaces. This may be
491 due to lower contact pressures in the hybrid-cartilage pairing either due to the reduced compressive
492 modulus of the hybrid compared with cartilage or the more conformal geometry of the hybrid-
493 cartilage system.

494 The hybrid material tested here is designed to biodegrade with time and be replaced by repaired
495 cartilage tissue. Dissolution studies of the material at 37°C in PBS have previously shown that over 7

496 days the material will release PCL, causing an increase in the inorganic/organic ratio [8], but it was
497 not known whether the rate of material dissolution would increase due to loading, or if changes in
498 the composition would impact the friction and wear performance of the material. Here TGA
499 measurements after 5 days in media at 37°C found the relative organic content of the hybrid
500 decreased by 1.4 wt% but the decrease due to friction testing was not significant ($\delta_{\text{wear}} = -0.2 \text{ wt\%}$)
501 when compared to the control that was soaked in the same media without friction testing ($\delta_{\text{soaking}} = -$
502 1.2 wt%). ICP-OES measurements showing a peak in Si release of $2.3 \pm 0.4 \mu\text{g mL}^{-1}$ at day 1 are
503 consistent with unloaded, soaked samples tested previously [8]. The combination of the TGA and
504 ICP-OES results suggest that over the 5 days of testing, as expected, both inorganic and organic
505 phases degraded at very slow rate, with a predominant loss of polymer. No changes in friction forces
506 or increases in GAG release were observed for the hybrid-cartilage testing pairs over the five day
507 testing period, suggesting that the release of small amounts of PCL does not affect the tribological
508 performance. There was also no difference in cell viability observed at the end of 5 days testing
509 which suggests any products released from the hybrid are non-toxic.

510 Although this is the first $\text{SiO}_2/\text{PTHF}/\text{PCL-diacid}$ hybrid material to be tested for cartilage repair
511 applications, some composite materials have previously been examined. Composite scaffolds
512 containing Bioglass particles have been suggested for osteochondral regeneration [5, 32], but with
513 no tribology or wear studies. A concern is that Bioglass® particles would be released which would
514 lead to mechanical damage of the cartilage surface through abrasive wear. Implants used to repair
515 focal defects that have metal bearing surfaces, that articulate against cartilage, can cause damage to
516 the opposing cartilage, and that the damage can be as severe as leaving the defect untreated [11,
517 12, 33]. Although often overlooked, tribological testing of proposed biomaterials for osteochondral
518 repair is a crucial part of the design process that will act as a safeguard against damaging devices and
519 will increase the chances of a successful translation into the clinic.

520 This study was designed to compare 5 different formulations of a new hybrid material and so a
521 simplified geometry and motion relative to that found in the human knee joint were used. Further
522 tests are needed to capture the effects of speed, cross-shear and variable loading on the tribological
523 properties or surface chemistry of the material. Although this study shows no increase in friction or
524 wear related to PCL degradation over a much longer time scale than other studies, it is still short of
525 the time needed for full breakdown of the material and growth of replacement cartilage tissue.
526 Longer term testing will build on these results and form part of the ongoing material development
527 process.

528

529 5. Conclusions

530 Here a SiO₂/PTHF/PCL-diCOOH hybrid material has been tested against a cartilage pin, to
531 discriminate between hybrid compositions and then tested in a more physiological conditions, using
532 a new bioreactor testing rig designed specifically to look at the friction and wear properties under
533 extreme conditions, to give an indication of *in vivo* performance. The silica content of the hybrid
534 material strongly affected the friction coefficient and hence shear force applied to the opposing
535 articular cartilage. The best frictional and wear properties were achieved through increasing the
536 silica content of the hybrid, although this must be balanced against introducing high contact
537 pressures which can be detrimental to cartilage tissue. After five days of testing against “living”
538 cartilage, no difference in friction or wear was seen for the hybrid rotating against cartilage pair
539 compared with the control cartilage-cartilage pairs. Wear of the hybrid was not observed despite a
540 reduction in the material PCL content over this period. This information will inform the development
541 of chondral and osteochondral scaffolds.

542

543 Acknowledgements

544 The authors acknowledge the European Commission funding under the 7th Framework Programme
545 (Marie Curie Innovative Training Network (ITN); grant number: 289958, Bioceramics for Bone
546 Repair); the EPSRC ((EP/K027549/1), EP/N025059/1) and National Institute for Health Global Health
547 Research (grant number 1613745: NIHR Group on POsT Conflict Trauma in Sri Lanka; ProTECT). Raw
548 data can be obtained from rdm-enquiries@imperial.ac.uk.

549 Epifluorescence images were obtained using equipment in the Facility for Imaging by Light
550 Microscopy (FILM) at Imperial College London, which is part supported by funding from the
551 Wellcome Trust (grant 104931/Z/14/Z) and BBSRC (grant BB/L015129/1). Raw data is available from
552 rdm-enquiries@imperial.ac.uk.

553 The authors would also like Marcus Wimmer, Robert Trevino and their colleagues at Rush University
554 who shared their design and experimental process for establishing a live cartilage-on-cartilage
555 testing platform.

556

557 **References**

- 558 [1] S.M. McNary, K.A. Athanasiou, A.H. Reddi, Engineering Lubrication in Articular Cartilage, *Tissue*
559 *Eng. Part B* 18(2) (2012) 88-100.
- 560 [2] I.M. Khan, S.J. Gilbert, S.K. Singhrao, V.C. Duance, C.W. Archer, Cartilage integration: evaluation
561 of the reasons for failure of integration during cartilage repair. A review, *Eur. Cells Mater.* 16 (2008)
562 26-39.
- 563 [3] H. Oonishi, L.L. Hench, J. Wilson, F. Sugihara, E. Tsuji, M. Matsuura, S. Kin, T. Yamamoto, S.
564 Mizokawa, Quantitative comparison of bone growth behavior in granules of Bioglass (R), A-W glass-
565 ceramic, and hydroxyapatite, *J. Biomed. Mater. Res.* 51(1) (2000) 37-46.
- 566 [4] J. Wilson, D. Noletti, Bonding of soft tissues to Bioglass®, in: T. Yamamuro, L.L. Hench, J. Wilson
567 (Eds.), *Handbook of Bioactive Ceramics*, CRC Press, Boca Raton, FL, 1990.
- 568 [5] Q.Q. Yao, P. Noeaid, R. Detsch, J.A. Roether, Y.M. Dong, O.M. Goudouri, D.W. Schubert, A.R.
569 Boccaccini, Bioglass (R)/chitosan-polycaprolactone bilayered composite scaffolds intended for
570 osteochondral tissue engineering, *J. Biomed. Mater. Res. Part A* 102(12) (2014) 4510-4518.
- 571 [6] J.R. Jones, Review of bioactive glass: From Hench to hybrids, *Acta Biomater* 9(1) (2013) 4457-
572 4486.
- 573 [7] B.M. Novak, Hybrid nanocomposite materials - between inorganic glasses and organic polymers,
574 *Adv. Mater.* 5(6) (1993) 422-433.
- 575 [8] F. Tallia, L. Russo, S. Li, A.L.H. Orrin, X. Shi, S. Chen, J.A.M. Steele, S. Meille, J. Chevalier, P.D. Lee,
576 M.M. Stevens, L. Cipolla, J.R. Jones, Bouncing and 3D printable hybrids with self-healing properties,
577 *Mater Horiz* 5 (2018) 849.
- 578 [9] G.R. Fulcher, D.W.L. Hukins, D.E.T. Shepherd, Viscoelastic properties of bovine articular cartilage
579 attached to subchondral bone at high frequencies, *Bmc Musculoskeletal Disorders* 10 (2009).

580 [10] M.A. Accardi, S.D. McCullen, A. Callanan, S. Chung, P.M. Cann, M.M. Stevens, D. Dini, Effects of
581 Fiber Orientation on the Frictional Properties and Damage of Regenerative Articular Cartilage
582 Surfaces, *Tissue Eng. Part A* 19(19-20) (2013) 2300-2310.

583 [11] R.J.H. Clusters, W.J.A. Dhert, M.H.P. van Rijen, A.J. Verbout, L.B. Creemers, D.B.F. Saris, Articular
584 damage caused by metal plugs in a rabbit model for treatment of localized cartilage defects,
585 *Osteoarthritis and Cartilage* 15(8) (2007) 937-945.

586 [12] R.J.H. Custers, W.J.A. Dhert, D.B.F. Saris, A.J. Verbout, M.H.P. van Rijen, S.C. Mastbergen, F.
587 Lafeber, L.B. Creemers, Cartilage degeneration in the goat knee caused by treating localized cartilage
588 defects with metal implants, *Osteoarthritis and Cartilage* 18(3) (2010) 377-388.

589 [13] M. Caligaris, G.A. Ateshian, Effects of sustained interstitial fluid pressurization under migrating
590 contact area, and boundary lubrication by synovial fluid, on cartilage friction, *Osteoarthritis and*
591 *Cartilage* 16(10) (2008) 1220-1227.

592 [14] E. Northwood, J. Fisher, A multi-directional in vitro investigation into friction, damage and wear
593 of innovative chondroplasty materials against articular cartilage, *Clinical Biomechanics* 22(7) (2007)
594 834-842.

595 [15] F. Li, Y.L. Su, J.P. Wang, G. Wu, C.T. Wang, Influence of dynamic load on friction behavior of
596 human articular cartilage, stainless steel and polyvinyl alcohol hydrogel as artificial cartilage, *J.*
597 *Mater. Sci. - Mater. Med.* 21(1) (2010) 147-154.

598 [16] S.M.T. Chan, C.P. Neu, K. Komvopoulos, A.H. Reddi, P.E. Di Cesare, Friction and Wear of
599 Hemiarthroplasty Biomaterials in Reciprocating Sliding Contact With Articular Cartilage, *Journal of*
600 *Tribology-Transactions of the Asme* 133(4) (2011).

601 [17] C.J. Bell, E. Ingham, J. Fisher, Influence of hyaluronic acid on the time-dependent friction
602 response of articular cartilage under different conditions, *Proceedings of the Institution of*
603 *Mechanical Engineers Part H-Journal of Engineering in Medicine* 220(H1) (2006) 23-31.

604 [18] M. Peroglio, D. Gaspar, D.I. Zeugolis, M. Alini, Relevance of bioreactors and whole tissue
605 cultures for the translation of new therapies to humans, *J. Orthop. Res.* 36(1) (2018) 10-21.

606 [19] R.L. Trevino, C.A. Pacione, A.M. Malfait, S. Chubinskaya, M.A. Wimmer, Development of a
607 Cartilage Shear-Damage Model to Investigate the Impact of Surface Injury on Chondrocytes and
608 Extracellular Matrix Wear, *Cartilage* 8(4) (2017) 444-455.

609 [20] M.A. Wimmer, S. Grad, T. Kaup, M. Hanni, E. Schneider, S. Gogolewski, M. Alini, Tribology
610 approach to the engineering and study of articular cartilage, *Tissue Eng.* 10(9-10) (2004) 1436-1445.

611 [21] S.J. Sweet, T. Takara, L. Ho, J.E. Tibone, Primary Partial Humeral Head Resurfacing Outcomes
612 With the HemiCAP Implant, *Am. J. Sports Med.* 43(3) (2015) 579-587.

613 [22] Z.G. Tang, R.A. Black, J.M. Curran, J.A. Hunt, N.P. Rhodes, D.F. Williams, Surface properties and
614 biocompatibility of solvent-cast poly epsilon-caprolactone films, *Biomaterials* 25(19) (2004) 4741-
615 4748.

616 [23] K.E. Strawhecker, S.K. Kumar, J.F. Douglas, A. Karim, The critical role of solvent evaporation on
617 the roughness of spin-cast polymer films, *Macromolecules* 34(14) (2001) 4669-4672.

618 [24] S. Graindorge, W. Ferrandez, E. Ingham, Z. Jin, P. Twigg, J. Fisher, The role of the surface
619 amorphous layer of articular cartilage in joint lubrication, *Proceedings of the Institution of*
620 *Mechanical Engineers Part H-Journal of Engineering in Medicine* 220(H5) (2006) 597-607.

621 [25] S. Kobayashi, S. Yonekubo, Y. Kurogouchi, Cryoscanning electron-microscopic study of the
622 surface amorphous layer of articular-cartilage, *Journal of Anatomy* 187 (1995) 429-444.

623 [26] M.R. Widmer, M. Heuberger, J. Voros, N.D. Spencer, Influence of polymer surface chemistry on
624 frictional properties under protein-lubrication conditions: implications for hip-implant design,
625 *Tribology Letters* 10(1-2) (2001) 111-116.

626 [27] M.P. Heuberger, M.R. Widmer, E. Zobeley, R. Glockshuber, N.D. Spencer, Protein-mediated
627 boundary lubrication in arthroplasty, *Biomaterials* 26(10) (2005) 1165-1173.

628 [28] J. Check, K.S.K. Karuppiah, S. Sundararajan, Comparison of the effect of surface roughness on
629 the micro/nanotribological behavior of ultra-high-molecularweight polyethylene (UHMWPE) in air
630 and bovine serum solution, *J. Biomed. Mater. Res. Part A* 74A(4) (2005) 687-695.

631 [29] B. Zappone, K.J. Rosenberg, J. Israelachvili, Role of nanometer roughness on the adhesion and
632 friction of a rough polymer surface and a molecularly smooth mica surface, *Tribology Letters* 26(3)
633 (2007) 191-201.

634 [30] C.T. Chen, M. Bhargava, P.M. Lin, P.A. Torzilli, Time, stress, and location dependent chondrocyte
635 death and collagen damage in cyclically loaded articular cartilage, *J. Orthop. Res.* 21(5) (2003) 888-
636 898.

637 [31] B.L. Wong, W.C. Bae, J. Chun, K.R. Gratz, M. Lotz, R.L. Sah, Biomechanics of cartilage
638 articulation, *Arthritis and Rheumatism* 58(7) (2008) 2065-2074.

639 [32] R.M. Day, A.R. Boccaccini, S. Shurey, J.A. Roether, A. Forbes, L.L. Hench, S.M. Gabe, Assessment
640 of polyglycolic acid mesh and bioactive glass for soft-tissue engineering scaffolds, *Biomaterials*
641 25(27) (2004) 5857-5866.

642 [33] A.H. Gomoll, H. Madry, G. Knutsen, N. van Dijk, R. Seil, M. Brittberg, E. Kon, The subchondral
643 bone in articular cartilage repair: current problems in the surgical management, *Knee Surgery Sports*
644 *Traumatology Arthroscopy* 18(4) (2010) 434-447.

645